BMB
Reports

BMB Rep. 2020; 53(7): 349-356
www.bmbreports.org

Invited Mini Review

Organic matrix-free imaging mass spectrometry

Eunjin Kim[#], Jisu Kim[#], Inseong Choi, Jeongwook Lee & Woon-Seok Yeo[*]
Department of Bioscience and Biotechnology, Bio/Molecular Informatics Center, Konkuk University, Seoul 05029, Korea

Mass spectrometry (MS) is an ideal tool for analyzing multiple types of (bio)molecular information simultaneously in complex biological systems. In addition, MS provides structural information on targets, and can easily discriminate between true analytes and background. Therefore, imaging mass spectrometry (IMS) enables not only visualization of tissues to give positional information on targets but also allows for molecular analysis of targets by affording the molecular weights. Matrix-assisted laser desorption/ionization-time of flight (MALDI-TOF) MS is particularly effective and is generally used for IMS. However, the requirement for an organic matrix raises several limitations that get in the way of accurate and reliable images and hampers imaging of small molecules such as drugs and their metabolites. To overcome these problems, various organic matrix-free LDI IMS systems have been developed, mostly utilizing nanostructured surfaces and inorganic nanoparticles as an alternative to the organic matrix. This minireview highlights and focuses on the progress in organic matrix-free LDI IMS and briefly discusses the use of other IMS techniques such as desorption electrospray ionization, laser ablation electrospray ionization, and secondary ion mass spectrometry. [BMB Reports 2020; 53(7): 349-356]

INTRODUCTION

In living organisms, the compositions of biomolecules such as proteins, nucleic acids, sugars, lipids, and metabolites change continuously and dynamically in response to a variety of environmental factors. The levels of these molecules in living tissues are precisely regulated to maintain homeostasis. Therefore, in many cases, the distribution of these molecules in tissues or cells can provide valuable information for basic biological research, diagnosis of certain diseases, and identification of therapeutic targets. Conventionally, the biodistribution of such molecules has been examined by cell/tissue 'homogenization' methods, which provide only biochemical information, not information on the spatial distribution of target molecules in tissues. On the contrary, spectroscopic visualizations such as fluorescence tissue imaging can reveal the spatial distribution of molecules; however, they do not allow for molecular analysis. For these reasons, imaging mass spectrometry (IMS) has been developed and extensively studied; IMS allows for both visualization of tissues to give positional information on targets and molecular analysis of targets by affording the molecular weights (1-3). In addition, the advantages of mass spectrometry (MS) are manifold: i) MS provides chemical and structural information on targets, ii) MS can easily discriminate between true analytes and background and, therefore, eliminate false positive signals, and iii) MS can be used to monitor multiple analytes simultaneously. Matrix-assisted laser desorption/ionization-time of flight (MALDI-TOF) MS is particularly effective and is generally used for IMS due to its suitability for tissue analysis and the 'soft' ionization of large biomolecules such as proteins and oligonucleotides (4, 5). In general, a solution of organic matrix, including 2,5-dihydroxybenzoic acid, sinapinic acid, α-cyano-4-hydroxycinnamic acid, and 2,4,6-trihydroxyacetophenone, depending on the types of analytes present, is deposited on a thin section of a tissue, which is then scanned by MALDI-TOF MS to give a raster image of the distribution of biomolecules as revealed by relative signal intensities. However, the requirement for an organic matrix limits the applicability of MALDI IMS. The signals in MALDI IMS, in many cases, are strongly affected by the choice of a proper matrix and solvents, co-crystallization of a matrix and analytes, and, particularly, homogeneity of matrix deposition, leading to poor shot-to-shot and sample-to-sample reliability. Therefore, peak intensities, i.e. raster images, would not represent the real spatial distribution of target molecules in tissues. In addition, the requirement for an organic matrix hampers imaging of small molecules such as drugs and their metabolites owing to interference of the matrix in the low-mass region. Thus, various organic matrix-free LDI IMS systems have been developed to avoid the problems described above, mostly utilizing nanostructured surfaces and inorganic nanoparticles (NPs) as an alternative to the organic matrix.

This minireview starts with a brief introduction to organic matrix-free LDI MS for small molecule analysis and focuses on the progress that has been made in organic matrix-free LDI IMS methods, which are categorized into i) nanostructured

*Corresponding author. Tel: +82-2-2049-6054; Fax: +82-2-454-8217; E-mail: wsyeo@konkuk.ac.kr
[#]These authors contributed equally to this work.

https://doi.org/10.5483/BMBRep.2020.53.7.078

Received 7 April 2020

Keywords: Imaging mass spectrometry, Nanoparticles, Nanostructured surfaces, Organic matrix-free

ISSN: 1976-670X (electronic edition)

surface-assisted LDI IMS and ii) inorganic nanoparticle-assisted LDI IMS. In addition, IMS methods using other 'soft' ionization methods such as desorption electrospray ionization (DESI) and laser ablation electrospray ionization (LAESI) will be discussed, followed by a brief discussion on the use of secondary ion mass spectrometry (SIMS), which have the advantages of little or no preparation, ease of implementation, and simplified analysis in ambient environments.

The main purpose of this minireview is to give the reader an unbiased description of the approaches for molecular level analyses of biological sample surfaces using MS, particularly for small molecules. This minireview, therefore, will not only offer a starting point for students and researchers entering this field but also be valued by active researchers requiring small molecule analyses of tissues in various areas including disease pathology, diagnostics, drug delivery systems, metabolomics, lipidomics, and pharmacokinetics.

ORGANIC MATRIX-FREE LDI MS

Organic matrix-free LDI MS mostly utilizes nanostructured surfaces and inorganic NPs and is known as surface-assisted LDI (SALDI) MS (6-8). SALDI materials transfer sufficient energy from the irradiated laser to analytes for desorption/ionization without damaging the analytes and causing fragmentation, and therefore have been used as matrices for analysis of small molecules. In addition, nanostructures of the SALDI materials can provide efficient loading capacities due to large surface area, and analytes can be concentrated on the NPs by ionic strength, hydrophobic interactions, covalent binding, or bio-specific interactions through surface modifications, resulting in high sensitivity (9). As a pioneering work, Siuzdak and co-workers reported desorption-ionization on a porous silicon (DIOS) surface which was produced from flat nanocrystalline silicon through a simple etching procedure (10). Small molecule analytes including peptides (*m/z* 500-2000), small organic molecules (*m/z* 150-650), and saccharides (*m/z* 200-350) can successfully be analyzed using an organic matrix-free format on a porous silicon surface. In addition to DIOS, tailored surfaces with nanostructures such as layer-by-layer films of gold nanoparticles (AuNPs) (11), Si nanowires (12), and graphite-coated films (13) have reportedly been used as nanostructured surfaces. Inspired by the first example by Tanaka *et al.*, in which 30 nm cobalt NPs mixed with glycerol were used as a matrix (4), various inorganic NPs including Au, Ag, Pt, SiO_2, TiO_2, Fe_2O_4, and ZnO have been widely used and examined for their compatibility in LDI MS (14). Particularly, AuNPs are most commonly used in biological studies owing to advantageous optical and physiochemical properties. There are pros and cons to using surface-type and particle-type organic matrix-free formats; for example, surface-type formats are robust and can be manufactured as a target plate for MALDI-TOF MS instruments, whereas particle-type formats facilitate protocol optimization for MS analysis and can act as a solid phase for extraction/enrichment of analytes in complex samples.

The following two sections describe organic matrix-free LDI IMS with grafting, the distinct feature of SALDI MS in small molecule analysis, as discussed above: i) nanostructured surfaces on which thin tissues are deposited, and ii) inorganic NPs which are sprayed onto thin tissues (Fig. 1).

NANOSTRUCTURED SURFACE-ASSISTED LDI IMS

Noncarbon-based surfaces

By utilizing the DIOS technique, which allows for small molecule analysis, Liu *et al*. accomplished imaging of small molecules in biological tissues at the cellular level on a porous silicon substrate (15). In that study, phosphatidylcholine in mouse liver tissue was analyzed by LDI MS, and then further indirect visualization of mammalian cells was demonstrated by constructing an ion map of the detected phosphatidylcholine. Rudd *et al*. investigated the biological role of two classes of secondary metabolites, brominated indoles and choline esters, in reproduction of Muricidae molluscs by observing changes in distribution of metabolites in mollusc tissue using DIOS (16, 17). IMS facilitated detection of the metabolites at different stages of the reproductive cycle of mature female *D. orbita*, one of molluscs, and proposed the biological roles of the metabolites based on temporal changes in their distribution. The DIOS substrates were further employed for the detection of drugs, lipids and metabolites (18, 19).

As an advanced use of DIOS, nanostructure initiator MS (NIMS) was introduced by the Siuzdak group for porous silicon-based mass analysis (20). NIMS uses a nanostructured silicon surface composed of roughly 10 nm pores to trap initiator molecules, such as fluorinated siloxane, lauric acid, and polysiloxane. The NIMS surface is exposed to laser irradiation resulting in vaporization or fragmentation of the initiator molecules and subsequent desorption/ionization of the absorbed analyte on the NIMS surface. The lipids (*m/z* 700-800) on the mouse embryo tissue section were visualized by NIMS (20), and this method was further extended to clinical applications for analysis of xenobiotics (*m/z* 200-350) and endogenous metabolites (*m/z* 150-350) in brain tissue and fluids with high sensitivity, no fragmentation, and no background interference (21). Although NIMS is well suited for the detec-

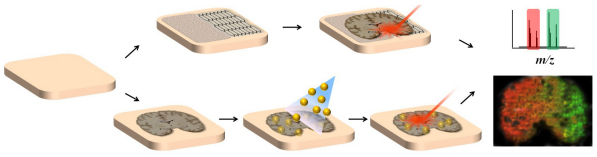

Fig. 1. LDI IMS with organic matrix-free systems harnessing nanostructured surfaces or nanoparticles.

tion of various biological molecules in tissues, detection of carbohydrates and steroids is challenging because of their poor ionization efficiency. For this reason, Patti *et al*. combined NIMS and spray deposition of NaCl or $AgNO_3$, which provided a uniform environment with a source of cations ($[M+Na]^+$ or $[M+Ag]^+$), for analysis of carbohydrates (*m/z* 180-400) and steroids (*m/z* 493) in *Gerbera jamesonii* stem and mouse brain tissue, respectively (22). This technique was further developed for imaging with essentially single-cell resolution, and NIMS was used to monitor drug exposure and metabolite biotransformation in single cells for the study of cancer metabolism (23). In addition, Ag films were sputter-coated thinly on porous silicon substrates, resulting in a dramatic improvement in the mass accuracy of fingerprint NIMS (24). For a discussion of the basic principles of NIMS for tissue imaging and various surface modifications and alternative nanostructured surfaces for NIMS, see the review by Calavia *et al*. (25).

Recently, Li *et al*. prepared a nanostructured surface consisting of a silver nanoisland on nanodiamonds which had a localized surface plasmon resonance wavelength very close to the laser wavelength of MALDI MS instruments, therefore demonstrating the enhanced efficiency of LDI for small molecule analysis (26). Those authors went on to apply the silver nanoisland surface to hexagonal boron nitride for IMS of ischemic brain damage with both small metabolites ($m/z > 500$) and sulfatides resulting in enhanced signal intensity of many small molecules and dramatic improvement in the visibility of raster images (27).

Carbon-based surfaces

In addition to porous silicon-based surfaces, carbon-based surfaces have also been used for matrix-free IMS. Many types of carbon-based materials, including functionalized carbon nanotubes and graphene oxides, have been suggested as alternative matrices for matrix-free IMS due to their absorption properties and efficient energy transfer to analytes. Kim *et al*. developed an LDI platform using a double layer of graphene oxide (GO) and aminated multi-walled carbon nanotube (MWCNT) for mouse brain tissue imaging (28). The deposition of aminated MWCNTs to the GO-coated surface yielded enhanced surface roughness and surface area for analyte adsorption, and, thus, increased LDI efficiency. This double layer effectively converted the absorbed UV light into thermal energy, allowing for imaging of glycerophosphocholine (*m/z* 800-860) and phosphatidylcholine (*m/z* 730-755) in mouse brain tissue as well as MS analysis of various biochemical small molecules. They also prepared multilayers of alternating MWCNT and GO and investigated the effect of thickness, assembly sequence, and surface roughness on LDI efficiency for small molecule analysis and IMS (29). Huang *et al*. demonstrated an interesting approach in which the protein mucin1, which is overexpressed in most adenocarcinomas, was utilized as a target for tumor cell analysis with LDI IMS (30). In their approach, a mucin1-binding aptamer was conjugated to AuNPs which were subsequently immobilized on a GO-coated surface. The resulting surface provided the mucin1-binding aptamers with ultrahigh density and high flexibility for cooperative and multivalent binding of mucin1 on cell membranes. By using LDI-MS to monitor Au cluster ions, four different mucin1 expression cell lines were analyzed on this surface, and this platform could be utilized further as a labeling agent for tumor tissue imaging. As additional carbon-based surfaces, a pulse laser-engineered functional graphene paper with graphitic nanospheres and a graphene-coated glass substrate combined with a continuous-wave laser for atmospheric pressure mass spectrometric analysis were demonstrated for IMS (31, 32).

NANOPARTICLE-ASSISTED LDI-IMS

Inorganic nanoparticles

The performance of inorganic NPs as matrices for LDI MS depends strongly on their size, morphology, composition, and concentration. In this respect, AuNPs and AgNPs are the most often studied and widely used materials in LDI-MS because their size is readily tunable and various shapes and compositions can be prepared depending on the researcher's purpose. Goto-Inoue *et al*. visualized the distribution and localization of glycosphingolipids ($m/z < 950$) – amphiphilic molecules involved in various biological processes – in mouse brain sections using AuNPs as a matrix (33). Compared with dihydroxybenzoic acid, a conventional organic matrix for glycosphingolipids, AuNPs provided approximately 20 times more sensitive detection of glycosphingolipids and successfully enabled visualization of ionic images of glycosphingolipids including 14 kinds of sulfatides and 10 kinds of gangliosides in mouse brain samples. Recently, Phan *et al*. compared three different sample preparation methods, including sublimation with two conventional organic matrices followed by recrystallization with trifluoroacetic acid, and surface modification with AuNPs to profile and image the lipids (*m/z* 500-900) in *Drosophila* brain tissue, which is an important model organism used in biological and neurological studies (34). They suggested that the different sample preparation methods made with a particular matrix material are suitable for detection of different biomolecules in the fly brain, and therefore, complementary analysis using a suitable matrix will allow for precise and diverse imaging of lipids in tissue samples.

AgNPs are also actively used for IMS. Hayasaka *et al*. harnessed AgNPs modified with alkylcarboxylate and alkylamine to visualize fatty acids ($m/z < 300$), such as stearic, oleic, linoleic, arachidonic, and eicosapentaenoic acid, and palmitic acid in mouse liver that are not detectable using a dihydroxybenzoic acid matrix (35). Additionally, they prepared mouse retinal tissue sections with a thickness of 10 μm and analyzed them with a scan pitch of 10 μm using AgNPs, revealing the six-zonal distribution of fatty acids in different layers of the retina. The Wood group introduced an AgNP

implantation method where AgNPs were formed with a magnetron and accelerated to 50 eV to be deposited across entire tissue sections for uniform and reproducible AgNP layer formation (36, 37). Gas phase AgNP ions were generated by magnetron sputtering and grown to 0.5-15 nm diameter, and then selected particles at 6 nm were implanted in the tissue section. This method produced high spatial resolution LDI images of various lipid species (*m/z* 600-1700) in rat heart and kidney tissues. Similarly, Dufresne *et al*. conducted simultaneous imaging of cholesterol along with olefins using metallic silver coatings at nanometer thicknesses with a sputter coating system (38). The Yeung group performed profiling and imaging of metabolites (*m/z* 400-700) on plant leaves, flowers, and roots by utilizing IMS with spray deposition of AgNPs (39, 40).

Since the first introduction of the graphite surface-assisted detection of proteolytic digests (*m/z* 150-1700) of cytochrome c by Sunner *et al*. (41), colloidal graphite materials have also been utilized for IMS. Yeung's group used an aerosol spray of colloidal graphite for the detection and localization of cerebrosides (*m/z* 800-880) in rat brain tissue (42) and small metabolites (*m/z* 130-450) such as organic acids, flavonoids, and oligosaccharides in fruits (43). Furthermore, they analyzed flavonoids (*m/z* 285-755) and cuticular waxes (*m/z* 280-615) in intact leaves of plants such as *Arabidopsis*, one of the most important model systems in plant biology (44).

Metal oxide nanoparticles

NPs of metal oxides have been utilized for SALDI materials due to their unique structures and compositions. The Setou group demonstrated IMS of lipids and peptides at cellular resolution (15 μm) using extremely small iron oxide NPs (3.7 nm in diameter) flanked by amorphous silicates with hydroxyl and amino groups on their surfaces (45). These hydrophilic functional groups facilitate the ionization of adsorbed analytes through not only efficient energy transfer but also preferential sodium/potassium adduct formation. This material was further used to determine the distribution of sulfatide (*m/z* $<$ 910) in the dentate gyrus region of the hippocampus (46). They also utilized TiO_2 NPs for LDI MS identification and visualization of low molecular weight metabolites in mouse brain tissue (47). In their work, IMS identification of the metabolites using TiO_2 NPs, AuNPs, and dihydroxybenzoic acid as matrix molecules were compared. While only 4 signals were specific to dihydroxybenzoic acid, 179 metabolites were specific to TiO_2 NPs. In addition, TiO_2 NPs provided a higher number of molecular signals than AuNPs without any NP-related peaks in visualization of mouse brain tissues.

Recently, metal oxide laser ionization (MOLI) MS was reported as an organic matrix-free system for lipid analysis using powders of various metal oxides such as ZnO, MgO, Fe_xO_y, Co_xO_y, and CuO as an alternative to organic matrices (48). In this method, lipid molecules were ionized by protonation or sodiation which can be attributed to Lewis acid-base interactions between analytes and metal oxide. As such, the MOLI MS method can offer a new approach for the analysis of lipids. For example, CaO as a matrix replacement provided reproducible lipid cleavage, enabling lipid profiling for bacterial identification (49, 50). MOLI MS was also applied to IMS by Basu *et al*., who used cerium(IV) oxide to induce laser-catalyzed fatty acyl cleavage for bacterial identification, and to detect and image fatty acids in brain tumor tissues (51).

OTHER IMS TECHNIQUES

Electrospray ionization-based IMS

The Cooks group first introduced the DESI method for analysis of diverse analytes including small non-polar compounds, peptides, and proteins (52). In this method, solvent microdroplets were electrosprayed onto the sample surface, and the impact of electrosprayed charged particles on the surface resulted in desorption and ionization of analytes. The resulting desorbed gas-phase ions were then transferred to a distant mass spectrometer which gave mass spectra similar to normal ESI MS. Using DESI MS, small molecule RDX (*m/z* 334) and coniceine (*m/z* 125) were observed on a porcine leather surface and *Conium maculatum* seed section, respectively. Furthermore, the same group carried out *in vivo* sampling of living tissue surfaces by analyzing the antihistamine loratadine on the human finger, suggesting that DESI can be used for IMS of biological materials in ambient conditions. As an expansion of DESI MS to IMS, the Cooks group reported the direct and specific determination of the distribution of epinephrine (*m/z* 184.1) and norepinephrine (*m/z* 170.1) along with various phospholipids (*m/z* 750-1000) in the porcine adrenal gland (53). In addition, localization of lipids in human prostate cancer and injured rat spiral cord tissue (54, 55) and secondary metabolites in plant materials (56) were also verified. Furthermore, three-dimensional images were constructed from a suitable set of two-dimensional images obtained using DESI IMS (57). For more details regarding DESI IMS, see the recent review by Parrot *et al*., which includes discussion of ionization mechanisms, sample preparations, and applications (58).

Another approach to electrospray ionization-based IMS, the combination of infrared (IR) laser ablation with electrospray ionization (LAESI), was introduced by the Vertes group (59). In LAESI-MS, biological and medical analytes and organisms with sufficient water content are analyzed using a mid-IR laser at 2940 nm, corresponding to the frequency of the O-H bond's vibration in water, resulting in strong absorption of the wavelength by the water. Because the sample absorbs mid-IR energy, a gas phase plume is created from the sample surface. These laser-ablated particulates from the sample surface then interact with electrospray droplets, which provide a source of ions, allowing ionization of the laser-ablated particulates and subsequent analysis by a detector. Using this method, excretion of the antihistamine fexofenadine (*m/z* 502.3) in urine samples of humans who had taken fexofenadine caplets orally was analyzed without the use of organic matrices (59). In ad-

dition, *in vivo* spatial metabolite profiling of French marigold seedlings was performed to observe the various metabolite peaks (*m*/*z* 150-770) on the leaf, stem, and root. As a further extension of this strategy for atmospheric pressure IMS, that group reported the distribution of various lipids (*m*/*z* 130-770) and metabolites (*m*/*z* 100-900) in mouse brain and plant leaf tissue sections (60, 61). The LAESI method was also applied for in situ profiling of metabolites in single cells, which is challenging due to the complexity and small size of the samples. Cells exhibit a large degree of metabolic diversity depending on age, nutrition, and environmental factors, and therefore, chemical imaging and analysis of individual cells in a cell population would have broad applicability in biomedical research and clinical diagnostics. The Vertes group utilized LAESI for metabolic profiling (62) and in situ cell-by-cell imaging (63) of single cells in different cell populations. The localization of various metabolites (m/z 100-650) was determined in onion and daffodil epidermal cells.

IMS with TOF-SIMS

SIMS is a desorption and ionization technique used to analyze the composition of surfaces by sputtering the surfaces with an energetic primary ion beam and analyzing secondary ions emitted from the surfaces (1, 64, 65). These secondary ions

Table 1. Analytical methods and target analytes discussed in this review

Analytical Method			Analyte	Imaging Target	Ref.
LDI-MS	DIOS	Porous silicon surface	Phosphatidylcholine (PC)	Mouse liver tissues, HEK 293 cells	15
			Metabolites	Molluscs tissues	16, 17
				Fingerprints	18, 19
	NIMS	Initiator coated surface	Lipids	Mouse embryo tissue	20
				Fingerprints	24
			Metabolites (Clozapine, Ketamine)	Mouse brain tissues	21
			Glucose, steroids	*Gerbera jamesonii* stem	22
			Cholesterol	Mouse brain tissues	23
	Carbon-based Surface	Graphene oxides, Carbon nanotubes	Glycerophosphocholine, phosphatidylcholine	Mouse brain tissues	29
			Mucin 1	Tumor tissues	30
			Adenine	Hippocampal tissues	32
	Inorganic NP	Au	Glycosphingolipids	Mouse brain tissues	33
			Lipids	Drosophila brain tissues	34
		Ag	Fatty acids	Mouse liver and retinal tissues	35
			Lipids	Rat heart tissues, Rat kidney tissues	36, 37, 38
			Metabolites	Plants (flower, root)	39, 40
		Fe_3O_4	Lipids, peptides	Rat cerebellum tissues	45
			Sulfatides	Rat hippocampal tissues	46
		TiO_2	Metabolites (putrescine, uracil, ornithine)	Mouse brain tissues	47
		Colloidal graphite	Proteolytic digests	Cytochrome *c*	41
			Cerebroside, metabolite, oligosaccharides	Rat brain tissues, fruits	42, 43
			Flavonoids, cuticular wax	Arabidopsis intact leaf	44
ESI-MS	DESI	Electrosprayed microdroplets	RDX, coniceine	Porcine leather, *Conum maculatum* seed	52
			Epinephrine, norepinephrine	Porcine adrenal gland	53
			Sulfatides, phosphatidylserine, phosphatidylinositol	Mouse brains	54, 55, 57
			Hyperforin, hypericin	Plant (leaf)	56
	LAESI	Infrared laser ablation	Fexofenadine (antihistamine)	Urine (human)	59
			Lipids	Rat brain tissues	61
			Metabolites	Plant (leaf)	60
				Epidermal cells	62, 63
SIMS		Primary ions	Lipopolysaccharides	Rat brain tissues	66
			Phosphocholine and Adenine	Single cells	69

can directly produce high-resolution chemical images, so this platform is well-suited for the analysis of surface composition of biological materials. Although LDI- and ESI-based methods are widely used for visualization of molecular distribution on biological surfaces due to their efficiency and simplicity, these methods produce limited-resolution raster images. In this respect, SIMS ionization is advantageous over these methods, as it allows not only high mass resolution but also high spatial resolution of low molecular weight analytes. In terms of spatial resolution, a commonly used LDI method is capable of resolution as small as 5-100 μm because it uses laser light which has a focused spot size as small as 1 μm. However, SIMS offers enhanced resolution because it uses a primary ion beam that can be focused as sharply as 10 nm, allowing IMS of single cells and even different organelles within cells. For example, Todd *et al*. reported organic ion imaging of rat brain tissues with an enhanced resolution using TOF-SIMS (66). In general, the monatomic primary ions (Ar^+, Ga^+, In^+, Au^+, Xe^+, Bi^+) are commonly used for SIMS, which sometimes causes extensive fragmentation of analytes, hampering highly sensitive IMS of tissue surfaces. This drawback can be overcome by using lower energetic polyatomic primary ion beams such as C_{60}^+, SF_5^+, Bi_3^+, Au_n^+, and Cs_n^+ for IMS, which does not result in extensive fragmentation (67, 68). Furthermore, TOF-SIMS has been successfully employed in 3-D IMS of biological systems. Fletcher *et al*. reported the visualization of cellular features and 3-dimensional mass spectral imaging using C_{60}^+ as a primary ion source (69). Phosphocholine and adenine in HeLa cells were detected and analyzed for MSI of single cells and identifying cellular organelles such as the nucleus and endoplasmic reticulum. Thus, TOF-SIMS can provide favorable conditions for tissue imaging as an alternative to LDI- and ESI-based IMS techniques owing to the highly enhanced resolution and capability of 3D imaging. On the other hand, TOF-SIMS suffers from the drawback of fragmentation of surface molecules and the high cost of equipment compared with LDI- and ESI-based facilities resulting in limited accessibility. Therefore, researchers must use caution when determining which analytical tools to use depending on the specifics of their biological samples and target molecules. Analytical methods and target analytes discussed in this review are summarized in Table 1.

ACKNOWLEDGEMENTS

This paper was supported by Konkuk University in 2017.

CONFLICTS OF INTEREST

The authors have no conflicting interests.

REFERENCES

1. Chughtai K and Heeren RMA (2010) Mass Spectrometric Imaging for Biomedical Tissue Analysis. Chem Rev 110, 3237-3277
2. Buchberger AR, DeLaney K, Johnson J and Li L (2018) Mass Spectrometry Imaging: A Review of Emerging Advancements and Future Insights. Anal Chem 90, 240-265
3. Xu X, Zhong J, Su Y, Zou Z, He Y and Hou X (2019) A brief review on mass/optical spectrometry for imaging analysis of biological samples. Appl Spectrom Rev 54:1, 57-85
4. Tanaka K, Waki H, Ido Y, Akita S, Yoshida Y and Yoshida T (1988) Protein and Polymer Analyses up to m/z 100 000 by Laser Ionization Time-of-flight Mass Spectrometry. Rapid Commun Mass Spectrom 2, 151-156
5. Karas M and Hillenkamp F (1988) Laser Desorption Ionziation of Proteins with Molecular Masses Exceeding 10,000 Daltons. Anal Chem 60, 2299-2301
6. Guinan T, Kirkbride P, Pigou PE, Ronci M, Kobus H and Voelcker NH (2015) Surface-assisted laser desorption ionization mass spectrometry techniques for application in forensics. Mass Spectrum Rev 34, 627-640
7. Law KP and Larkin JR (2011) Recent advances in SALDI-MS techniques and their chemical and bioanalytical applications. Anal Bioanal Chem 399, 2597-2622
8. Chiang CK, Yang Z, Lin YW, Chen WT, Lin HJ and Chang HT (2010) Detection of Proteins and Protein-Ligand Complexes Using HgTe Nanostructure Matrixes in Surface-Assisted Laser Desorption/Ionization Mass Spectrometry. Anal Chem 82, 4543-4550
9. Chiang NC, Chiang CK, Lin ZH, Chiu TC and Chang HT (2009) Detection of aminothiols through surface-assisted laser desorption/ionization mass spectrometry using mixed gold nanoparticles. Rapid Commun Mass Spectrom 23, 3063-3068
10. Wei J, Bruiak JM and Siuzdak G (1999) Desorption-ionization mass spectrometry on porous silicon. Nature 399, 243-246
11. Kawasaki H, Sugitani T, Watanabe T, Yonewawa T, Moriwaki H and Arakawa R (2008) Layer-by-Layer Self-Assembled Mutilayer Films of Gold Nanoparticles for Surface-Assisted Laser Desorption/Ionization Mass Spectrometry. Anal Chem 80, 7524-7533
12. Luo G, Chen Y, Daniels H, Dubrow R and Vertes A (2006) Internal energy Transfer in Laser Desorption/Ionization form Silicon Nanowires. J Phys Chem B 110, 13381-13386
13. Kawasaki H, Takahashi N, Fujimori H et al (2009) Functionalized pyrolytic highly oriented graphite polymer film for surface-assisted laser desorption/ionization mass spectrometry in environmental analysis. Rapid Commun Mass Spectrom 23, 3323-3332
14. Chiang CK, Chen WT and Chang HT (2010) Nanoparticle-based mass spectrometry for the analysis of biomolecules. Chem Soc Rev 40, 1269-1281
15. Liu Q, Guo Z and He L (2007) Mass Spectrometry Imaging of Small Molecules Using Desorption/Ionization on Silicon. Anal Chem 79, 3535-3541
16. Rudd D, Ronci M, Johnston MR, Guinan T, Voelcker NH and Benkendorff K (2015) Mass spectrometry imaging reveals new biological roles for choline esters and Tyrian

purple precursors in muricid molluscs. Sci Rep 5, 13408
17. Ronci M, Rudd Dm, Guinan T, Benkendorff K and Voelcker NH (2012) Mass Spectrometry Imaging on Porous Silicon: Investigating the Distribution of Bioactives in Marine Mollusc Tissues. Anal Chem 84, 8996-9001
18. Guinan T, Vedova CD, Kobus H and Voelcker NH (2015) Mass spectrometry imaging of fingerprint sweat on nanostructured silicon. Chem Commun 51, 6088-6091
19. Gustafsson OJR, Guinan TM, Rudd D, Kobus H, Benkendorff K and Voelcker NH (2017) Metabolite mapping by consecutive nanostructure and silver-assisted mass spectrometry imaging on tissue sections. Rapid Commun Mass Spectrom 31, 991-1000
20. Northen TR, Yanes O, Northen MT et al (2007) Clathrate nanostructures for mass spectrometry. Nature 449, 1033-1036
21. Yanes O, Woo HK, Northen TR et al (2009) Nanostructure Initiator Mass Spectrometry: Tissue Imaging and direct Biofluid Analysis. Anal Chem 81, 2969-2975
22. Patti GJ, Woo HK, Yanes O et al (2010) Detection of Carbohydrates and Steroids by Cation-Enhanced Nanostructure-Initiator Mass Spectrometry (NIMS) for Biofluid Analysis and Tissue Imaging. Anal Chem 82, 121-128
23. O'Brien PJ, Lee M, Spilker ME et al (2013) Monitoring metabolic responses to chemotherapy in single cells and tumors using nanostructure-initiator mass spectrometry (NIMS) imaging. Cancer Metabol 1, 4
24. Guinan TM, Gustafsson OJR, McPhee G, Kobus H and Voelcker NH (2015) Silver Coating for High-Mass-Accuracy Imaging Mass Spectrometry of Fingerprints on Nanostructured Silicon. Anal Chem 87, 11195-11202
25. Calavia R, Annanouch FE, Correig X and Yanes O (2012) Nanostructure Initiator Mass Spectrometry for tissue imaging in metabolomics: Future prospects and perspectives. J Proteom 75, 5061-5068
26. Li Y, Cao X, Zhan L et al (2018) Hot electron transfer promotes ion production in plasmonic metal nanostructure assisted laser desorption ionization mass spectrometry. Chem Commun 54, 10905-10908
27. Li Y, Luo P, Cao X et al (2019) Enhancing surface-assisted laser desorption ionization mass spectrometry performance by integrating plasmonic hot-electron transfer effect through surface modification. Chem Commun 55, 5769-5772
28. Kim YK, Na HK, Kwack SJ et al (2011) Synergistic Effect of Graphene Oxide/MWCNT Films in Laser Desorption/Ionization Mass Spectrometry of Small Molecules and Tissue Imaging. ACS Nano 5, 4550-4561
29. Kim YK and Min DH (2012) Fabrication of Alternating Multilayer Films of Graphene Oxide and Carbon Nanotube and Its Application in Mechanistic Study of Laser Desorption/Ionization of Small Molecules. ACS Appl Mater Interfaces 4, 2088-2095
30. Huang RC, Chiu WJ, Lai IPJ and Huang CC (2015) Multivalent Aptamer/Gold Nanoparticle–Modified Graphene Oxide for Mass Spectrometry–Based Tumor Tissue Imaging. Sci Rep 5, 10292
31. Qian K, Zhou L, Liu J et al (2013) Laser Engineered Graphene Paper for Mass Spectrometry Imaging. Sci Rep 3, 1415
32. Kim JY, Lim H, Lee SY et al (2019) Graphene-Coated Glass Substrate for Continuous Wave Laser Desorption and Atmospheric Pressure Mass Spectrometric Imaging of a Live Hippocampal Tissue. ACS Appl Mater Interfaces 11, 27153-27161
33. Goto-Inoue N, Hayasaka T, Zaima N et al (2010) The Detection of Glycosphingolipids in Brain Tissue Sections by Imaging Mass Spectrometry Using Gold Nanoparticles. J Am Soc Mass Spectrom 21, 1940-1943
34. Phan NTN, Mohammadi AS, Pour MD and Ewing AG (2016) Laser Desorption Ionization Mass Spectrometry Imaging of Drosophila Brain Using Matrix Sublimation versus Modification with Nanoparticles. Anal Chem 88, 1734-1741
35. Hayasaka T, Goto-Inoue N, Zaima N et al (2010) Imaging Mass Spectrometry with Silver Nanoparticles Reveals the Distribution of Fatty Acids in Mouse Retinal Sections. J Am Soc Mass Spectrom 21, 1446-1454
36. Jackson SN, Baldwin K, Muller L et al (2014) Imaging of lipids in rat heart by MALDI-MS with silver nanoparticles. Anal Bioanal Chem 406, 1377-1386
37. Muller L, Kailas A, Jackson SN et al (2015) Lipid imaging within the normal rat kidney using silver nanoparticles by matrix-assisted laser desorption/ionization mass spectrometry. Kidney Int 88, 186-192
38. Dufresne M, Thomas A, Breault-Turcot J, Masson JF and Chaurand P (2013) Silver-Assisted Laser Desorption Ionization For High Spatial Resolution Imaging Mass Spectrometry of Olefins from Thin Tissue Sections. Anal Chem 85, 3318-3324
39. Cha S, song Z, Nikolau BJ and Yeung ES (2009) Direct Profiling and Imaging of Epicuticular Waxes on *Arabidopsis thaliana* by Laser Desorption/Ionization Mass Spectrometry Using Silver Colloid as a Matrix. Anal Chem 81, 2991-3000
40. Jun JH, Song Z, Liu Z et al (2010) High-Spatial and High-Mass Resolution Imaging of Surface Metabolites of *Arabidopsis thaliana* by Laser Desorption-Ionization Mass Spectrometry Using Colloidal Silver. Anal Chem 82, 3255-3265
41. Sunner J, Dratz E and Chen YC (1995) Graphite Surface-Assisted Laser Desorption/Ionization Time-of-Flight Mass Spectrometry of Peptides and Proteins from Liquid Solutions. Anal Chem 67, 4335-4342
42. Cha S and Yeung ES (2007) Colloidal Graphite-Assisted Laser Desorption/Ionization Mass Spectrometry and MS^n of Small Molecules. 1. Imaging of Cerebrosides Directly from Rat Brain Tissue. Anal Chem 79, 2373-2385
43. Zhang H, Cha S and Yeung ES (2007) Colloidal Graphite-Assisted Laser Desorption/Ionization MS and MS^n of Small Molecules. 2. Direct Profiling and MS Imaging of Small Metabolites from Fruits. Anal Chem 79, 6575-6584
44. Cha S, Zhang H, Iiarslan HI et al (2008) Direct profiling and imaging of plant metabolites in intact tissues by using colloidal graphite-assisted laser desorption ionization mass spectrometry. Plant J 55, 348-360
45. Taira S, Sugiura Y, Moritake S, Shimma S, Ichiyanagi Y and Setou M (2008) Nanoparticle-Assisted Laser Desorption/Ionization Based Mass Imaging with Cellular Resolution. Anal Chem 80, 4761-4766

46. Ageta H, Asai S, Sugiura Y, Goto-Inoue N, Zaima N and Setou M (2009) Layer-specific sulfatide localization in rat hippocampus middle molecular layer is revealed by nanoparticle-assisted laser desorption/ionization imaging mass spectrometry. Med Mol Morphol 42, 16-23
47. Shrivas K, Hayasaka T, Sugiura Y and Setou M (2011) Method for Simultaneous Imaging of Endogenous Low Molecular Weight Metabolites in Mouse Brain Using TiO2 Nanoparticles in Nanoparticle-Assisted Laser Desorption/Ionization-Imaging Mass Spectrometry. Anal Chem 83, 7283-7289
48. McAlpin CR, Voorhees KJ, Corpuz AR and Richards RM (2012) Analysis of Lipids: Metal Oxide Laser Ionization Mass Spectrometry. Anal Chem 84, 7677-7683
49. Voorhees KJ, McAlpin CR and Cox CR (2012) Lipid profiling using catalytic pyrolysis/metal oxide laser ionization-mass spectrometry. J Anal Appl Pyrol 98, 201-206
50. Voorhees KJ, Jensen KR, McAlpin CR et al (2013) Modified MALDI MS fatty acid profiling for bacterial identification. J Mass Spectrom 48, 850-855
51. Basu SS, McMinn MH, Lopez BGC et al (2019) Metal Oxide Laser Ionization Mass Spectrometry Imaging (MOLI MSI) Using Cerium(IV) Oxide. Anal Chem 91, 6800-6807
52. Takats Z, Wiseman JM, Gologan B, Cooks RG (2004) Mass Spectrometry Sampling Under Ambient Conditions with Desorption Electrospray Ionization. Science 306, 471-473
53. Wu C, Ifa DR, Manicke NE and Cooks RG (2009) Molecular imaging of adrenal gland by desorption electrospray ionization mass spectrometry. Analyst 135, 28-32
54. Eberlin LS, Dill AL, Costa AB et al (2010) Cholesterol Sulfate Imaging in Human Prostate Cancer Tissue by Desorption Electrospray Ionization Mass Spectrometry. Anal Chem 82, 3430-3434
55. Girod M, Shi Y, Cheng JX and Cooks RG (2011) Mapping Lipid Alterations in Traumatically Injured Rat Spinal Cord by Desorption Electrospray Ionization Imaging Mass Spectrometry. Anal Chem 83, 207-215
56. Thunig J, Hansen SH and Janfelt C (2011) Analysis of Secondary Plant Metabolites by Indirect Desorption Electrospray Ionization Imaging Mass Spectrometry. Anal Chem 83, 3256-3259
57. Eberlin LS, Ifa DR, Wu C and Cooks RG (2010) Three-Dimensional Vizualization of Mouse Brain by Lipid Analysis Using Ambient Ionization Mass Spectrometry. Angew Chem Int Ed 49, 873-876
58. Parrot D, Papazian S, Foil D, Tasdemir D (2017) Imaging the Unimaginable: Desorption Electrospray Ionization-Imaging Mass Spectrometry (DESI-MS) in Natural Product Research. Planta Med 84, 584-593
59. Nemes P and Vertes A (2007) Laser Ablation Electrospray Ionization for Atmospheric Pressure, in Vivo, and Imaging Mass Spectrometry. Anal Chem 79, 8098-8106
60. Nemes P, Barton AA and Vertes A (2009) Three-Dimensional Imaging of Metabolites in Tissues under Ambient Conditions by Laser Ablation Electrospray Ionization Mass Spectrometry. Anal Chem 81, 6668-6675
61. Nemes P, Woods AS and Vertes A (2010) Simultaneous Imaging of Small Metabolites and Lipids in Rat Brain Tissues at Atmospheric Pressure by Laser Ablation Electrospray Ionization Mass Spectrometry. Anal Chem 82, 982-988
62. Shrestha B and Vertes A (2009) In Situ Metabolic Profiling of Single Cells by Laser Ablation Electrospray Ionization Mass Spectrometry. Anal Chem 81, 8265-8271
63. Shrestha B, Patt JM and Vertes A (2011) In Situ Cell-by-Cell Imaging and Analysis of Small Cell Populations by Mass Spectrometry. Anal Chem 83, 2947-2955
64. Bletsos IV and Hercules DM (1985) Time-of-Flight Secondary Ion Mass Spectrometry of Nylons: Detection of High Mass Fragments. Anal Chem 57, 2384-2388
65. Niehuis E, Heller T, Feld H and Benninhoven A (1987) Design and performance of a reflectron based time-of-flight secondary ion mass spectrometer with electrodynamic primary ion mass separation. J Vac Sci Technol A 5, 1243-1246
66. Todd PJ, Schaaff TG, Chaurand P and Caprioli RM (2001) Organic ion imaging of biological tissue with secondary ion mass spectrometry and matrix-assisted laser desorption/ionization. J Mass Spectrom 36, 355-369
67. Weibel D, Wong S, Lockyer N, Blenkinsopp P, Hill R and Vickerman JC (2003) A C60 Primary Ion Beam System for Time of Flight Secondary Ion Mass Spectrometry: Its Development and Secondary Ion Yield Characteristics. Anal Chem 75, 1754-1764
68. McDonnell LA and Heeren RMA (2007) IMAGING MASS SPECTROMETRY. Mass Spectrom Rev 26, 606-643
69. Fletcher JS, Rabbani S, Henderson A, Lockyer NP and Vickerman JC (2011) Three-dimensional mass spectral imaging of HeLa-M cells-sample preparation, data interpretation and visualisation. Rapid Commun Mass Spectrom 25, 925-932